

## Molecular Packing of Amphiphiles with Crown Polar Heads at the Air–Water Interface

K. Larson,<sup>†</sup> D. Vaknin,<sup>‡</sup> O. Villavicencio,<sup>§</sup> D. McGrath,<sup>§</sup> and V. V. Tsukruk<sup>\*,†</sup>

Department of Materials Science and Engineering, Iowa State University, Ames, Iowa 50011, Ames Laboratory and Department of Physics and Astronomy, Iowa State University, Ames, Iowa 50011, and Department of Chemistry, University of Arizona, P.O. Box 210041, Tucson, Arizona 85721

Received: November 6, 2001; In Final Form: February 22, 2002

An amphiphilic compound containing a benzyl-15-crown-5 focal point, azobenzene spacer, and a dodecyl tail as a peripheral group has been investigated at the air–water interface. X-ray reflectivity and grazing incident diffraction (XGID) were performed on the Langmuir monolayers to elucidate molecular packing and orientation of molecular fragments for the compound with mismatch between cross-sectional areas of hydrophobic and hydrophilic segments. At high surface pressure, we observed intralayer packing of the alkyl tails with doubling parameters of the conventional orthorhombic unit cell (supercell) and long-range positional ordering. High tilt of the alkyl tails of 58° from the surface normal was a signature of molecular packing caused by a large mismatch between the cross-sectional areas of the polar head (45 Å<sup>2</sup>) and the alkyl tail (20 Å<sup>2</sup>).

## Introduction

Interfacial behavior of amphiphilic monodendrons is an intriguing topic in the field of organized molecular films. The mismatch of cross-sectional areas between polar heads and dendritic shells with multiple alkyl-terminated branches (Figure 1) determines their nontrivial packing structure and physical behavior as monolayers at solid and liquid surfaces.<sup>1–5</sup> It has been proven that the change of the dendritic shell with generation number governs the overall shape of the monodendrons for high generations.<sup>6,7</sup> The multiple alkyl tails give rise to steric hindrance that limits mobility of the polymer backbone and its ability to adapt a tree-like branching structure.<sup>8–10</sup> The shape of the periphery tails (length, flexibility, bulkiness) determines the ultimate shape of the individual monodendrons. Recently, we have introduced monodendrons with bulky polar heads and photochromic fragments and observed that the photochromic behavior of the Langmuir monolayers was, in fact, controlled by this cross-sectional mismatch.<sup>11–13</sup>

Much less attention has been paid to the role of the focal group in the overall shape of the monodendrons. Recent studies have focused on three-, four-, and six-tailed monodendrons that contain different polar heads.<sup>14</sup> It has been observed that the cross-sectional mismatch between the dendritic core and terminal branches can play a critical role in the overall shape of the molecules and their dense packing at the interfaces. This can be even more important in molecules with large differences between the cross-sectional areas of the focal group and terminal branches where the mismatch favors the dense packing of the polar heads against the alkyl tails. The variation of such steric hindrance influences the packing of the tails. In the case when the cross-sectional area of the polar heads is significantly larger than that of the hydrophobic tail, the availability of free space may lead to a disordered state of the flexible alkyl tails.

\* To whom correspondence should be addressed. E-mail: Vladimir@iastate.edu.

<sup>†</sup> Department of Materials Science and Engineering, Iowa State University.

<sup>‡</sup> Department of Physics and Astronomy, Iowa State University.

<sup>§</sup> Department of Chemistry, University of Arizona.

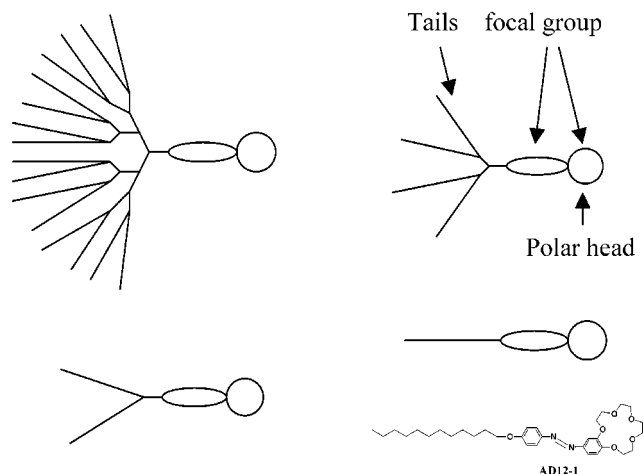


**Figure 1.** Sketches of monodendrons with multiple tails and a focal point along with “scaling down” to the current molecule **AD12–1** with one alkyl tail. Chemical structure is presented for **AD12–1**.

In the present communication, we report on the first results of direct structural studies of Langmuir monolayers fabricated from amphiphilic molecules with a bulky polar headgroup and a single alkyl tail such as presented in Figure 1. This molecule represents a limiting situation when the cross-sectional area of the bulk polar group (about 45 Å<sup>2</sup>) is twice that of the terminal alkyl chain (close to 20 Å<sup>2</sup>). The type of molecular ordering/disordering of the alkyl tails under these extreme conditions of abundant space available at the air–water interface for alkyl tails is a focus of the current study. The variation of molecular packing for these molecules with more than one alkyl tail or higher generation monodendrons such as cartooned in Figure 1 (two, four, and eight tails) is a subject of current investigation and will be published elsewhere.<sup>15</sup>

## Experimental Section

The **AD12–1** molecule presented in Figure 1 consists of a large crown ether head attached to an azobenzene group, and

has a single twelve-carbon alkyl tail attached to the opposite end of the azobenzene.<sup>11,12</sup> Monomolecular films at the air–water interface were prepared by the Langmuir technique on a temperature-controlled, Teflon trough. The monolayers were prepared from a chloroform solution (Fisher, reagent grade) with a concentration of 1.0 mmol/L. The solution was spread over a pure water subphase (Nanopure, > 18M $\Omega$  cm). The monolayer was allowed to stay at the air/water interface for 20 min to allow for the evaporation of the spreading solvent before compression. The monolayer was compressed at a rate of 1.2  $\text{\AA}^2/\text{min}$  until the desired pressure was reached. During the synchrotron experiments, the trough was purged with helium to reduce the background scattering from air and prevent damage from the oxidation of the monolayer.

A combination of X-ray grazing incident diffraction (XGID) (in-plane and rod-scans) and X-ray reflectivity measurements was used to characterize the monolayer structure according to the known approach.<sup>16–18</sup> Experiments were conducted on the Ames Laboratory liquid-surface diffractometer at the 6ID beam line at the Advanced Photon Source synchrotron at Argonne National Laboratory. Details regarding X-ray reflectivity and XGID and the experimental setup are described elsewhere.<sup>19</sup> A downstream Si double crystal monochromator was used to select the X-ray beam at the desired energy ( $\lambda = 0.772 \text{ \AA}$ ). After slow compression and relaxation, the monolayer was held at a constant pressure for the duration of the measurements.

The box model was used to determine the electron densities across the interface and to relate them to the molecular arrangements of the molecular fragments at the interface.<sup>20</sup> The box model consists of slabs of differing thickness and electronic density stacked above the water subphase with known electron density (0.33  $\text{e}/\text{\AA}^3$ ). The interfaces are smeared to account for the surface roughness and thermal vibrations. The arrangement of the molecular segments can be determined from the length and electron density of the boxes via direct comparison with molecular models. The reflectivity used to fit the experimental data was calculated from

$$R(Q_z) = R_0(Q_z)e^{-Q_z\sigma^2} \quad (1)$$

where the  $R_0(Q_z)$  is the reflectivity from steplike functions and  $\sigma$  is the surface roughness. The reflectivity calculated for various trial electronic density profiles was compared with experimental results during the fitting procedure.

Rod scans along the surface normal at the 2D Bragg's reflections were measured to determine the form factor of the diffracting objects. The intensity was quantitatively analyzed along the 2D Bragg reflection rod by using the framework of the distorted wave Born approximation (DWBA)<sup>21</sup>

$$I \propto |t(k_{z,f})|^2 |F(Q_z)|^2 \quad (2)$$

where  $t(k_{z,f})$  is the Fresnel transmission function, which gives rise to the enhancement around the critical angle of the scattered beam. The alkyl tails were modeled as cylinders of a length  $l$  and a fixed radius equal to the cross-sectional radius of alkyl chains. In modeling, the rod scans the length and tilt of the tails were varied, and the intensity were adjusted for two tilt directions: one toward nearest neighbors (NN) and the second toward next NN (NNN).<sup>22</sup> The form factor for the tails is given by

$$F(Q_z') = \sin(Q_z'l/2)/(Q_z'l/2) \quad (3)$$

where  $Q_z'$  is defined along the long axis of the tail.

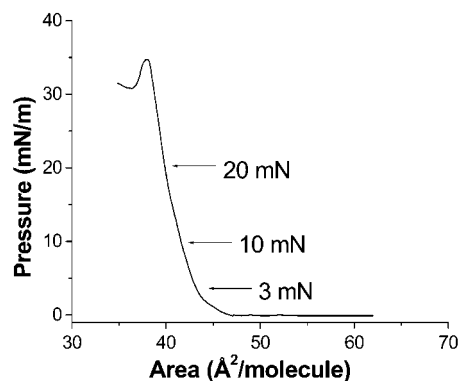


**Figure 2.** The  $\pi$ - $A$  isotherm for AD12-1. The surface pressures used in the X-ray experiments are labeled.

Molecular models were built with a Cerius<sup>2</sup> 3.8 package on a SGI workstation by using the Dreiding 2.21 force field library. Molecular models were treated with a molecular dynamics and a minimization procedure to obtain conformations with minimal energy. The alkyl tails were densely packed in the unit cell using parameters deduced from experimental data to analyze possible steric restrictions and the ability of the molecules to adapt the molecular packing proposed.

## Results and Discussion

The  $\pi$ - $A$  isotherm obtained for the compound studied displayed a gradual increase of surface pressure during lateral compression up to point of collapse (Figure 2). It indicates a solid monolayer being formed at the molecular area below 45  $\text{\AA}^2$ . From the isotherm, the molecular area in the solid state can be determined according to usual procedure to be 40–43  $\text{\AA}^2$ .<sup>23</sup> This value is twice the cross-sectional area of closely packed alkyl tails of about 20  $\text{\AA}^2$ .<sup>24</sup> Using molecular modeling, the cross-sectional area of the bulky polar head in planar conformation was calculated to be 45  $\text{\AA}^2$ . The sharp increase in surface pressure for molecular areas below 43  $\text{\AA}^2$  indicates that the large polar heads determine the dense packing of the molecules at the air–water interface and not the alkyl tail. Apparently, under these conditions, at low surface pressure, the alkyl tails cannot appear to be densely packed in a conventional manner and should adapt completely disordered state. X-ray reflectivity and XGID measurements can yield a detailed picture of the molecular packing of the alkyl tails under the condition of a large mismatch.

The experimental reflectivity data of AD12-1 at three different pressures is shown in Figure 3. At the lowest surface pressure, we observed diffuse reflectivity with a poorly visible first minimum. Increasing the surface pressure to 20 mN/m (compressed solid state of the monolayer) resulted in a much sharper first minimum and a weak second minimum. This indicates more ordered packing of the molecular fragments at higher pressures. The experimental reflectivity data can be analyzed by using a two-box model of the density distribution along the surface normal with variable length, density, and roughness of the boxes. It is worth to note that the distinction between the crown ether and azobenzene fragment could not be resolved within current resolution, and thus, we assigned one box to the alkyl tail and a second one to the azobenzene-crown fragment. An example of the best fit to the measured reflectivity with a smeared and unsmeared (i.e., zero surface roughness) density distribution is presented in Figure 3b as obtained from the analysis of the X-ray reflectivity data at the highest surface pressure.

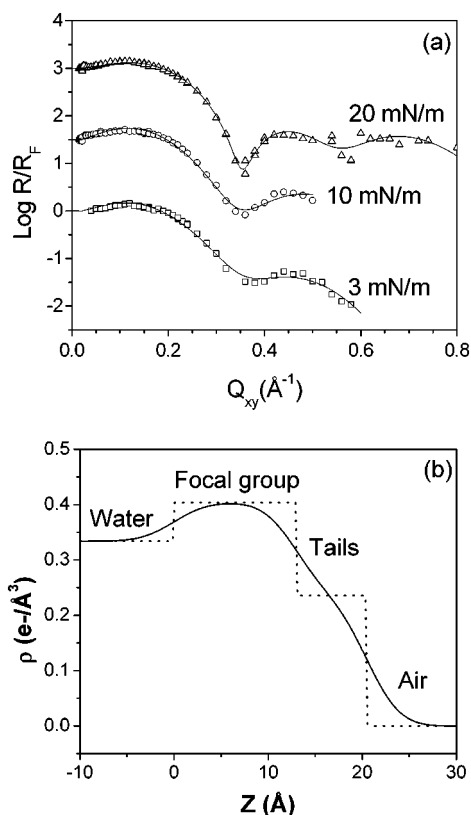


**Figure 3.** (a) X-ray reflectivity data and corresponding best fit plots for the AD12–1 monolayer at all three surface pressures. The symbols represent the experimental data, whereas the solid lines are simulations for the best electron density distribution profiles. (b) The two-box models with sharp interfaces and corresponding smeared electronic density distribution along the normal to the surface plane as obtained for the highest pressure.

**TABLE 1: Structural Parameters of Monolayers Deducted for Fitting Reflectivity Data with the Two Box Models for Different Surface Pressures**

| pressure (mN/m)                 | 3     | 10   | 20              |
|---------------------------------|-------|------|-----------------|
| head density ( $e/\text{Å}^3$ ) | 0.42  | 0.44 | $0.41 \pm 0.03$ |
| head length (Å)                 | 17.8  | 18.2 | $12.9 \pm 4.0$  |
| tail density ( $e/\text{Å}^3$ ) | 0.075 | 0.10 | $0.24 \pm 0.05$ |
| tail length (Å)                 | 9.1   | 8.7  | $7.5 \pm 2.0$   |
| roughness (Å)                   | 3.9   | 3.5  | $2.7 \pm 0.3$   |

Table 1 shows the structural parameters of the monolayer obtained for the different surface pressures from our simulations. As is clear seen from these data, the length of the polar fragment and its packing density varies insignificantly at the lower pressures. The total number of electrons per unit cell can be estimated from:  $N_{\text{REF}} = A \int \rho(z) dz$ , where  $A$  is the molecular area extracted from the  $\pi$ - $A$  isotherm. The entire molecule showed little increase of electrons over the molecular model but the densities of the individual boxes show large variations not entirely explained by the experimental uncertainty. Using this procedure, the estimated number of electrons for the polar head box is larger by 22 electrons than the number calculated from the chemical composition. Our suggestion is that this difference indicates approximately two water molecules can be located in proximity to the crown ether and the azobenzene. The partial hydration of the polar heads and azobenzenes explains the difference between the expected electronic density ( $0.37 e/\text{Å}^3$ ) and the observed density ( $0.41 e/\text{Å}^3$ ). Indeed, Pao et al. found that crown ether hydrophilic cores are packed below the water surface.<sup>25</sup> In addition, they observed a low-density region between the water surface and the densely packed alkyl

chains for monodendrons with multiple alkyl tails. In our case of only one alkyl tail, we find no low-density region between the crown heads and the alkyl tails despite the cross-sectional mismatch. Obviously, that absence of a bulk junction of several branches facilitates smooth density distribution from the polar fragment to the alkyl tail layer. From the reflectivity data we can also estimate that the crown ether head and photochromic group are tilted  $48^\circ$  from the surface normal (Table 1). This last result suggests that the overall conformation of the molecule is not straightforward but includes a “kink” in the middle of the molecule with the angle between two segments of about  $10^\circ$ . This differs by only a few degrees to the angle suggested from molecular modeling of these molecules.<sup>13</sup>

Very low electron density of the alkyl tails at the lower surface pressures of 3 and 10 mN/m (Table 1) clearly indicates that they are loosely packed and disordered at these surface pressures as is confirmed by diffraction data (see below). Density of alkyl layer increases significantly at the highest surface pressure indicating significant improvement of chain packing. However, even at the highest pressure studied here, the density of the alkyl tails extracted from the model ( $0.24 \pm 0.05 e/\text{Å}^3$ ) is lower than the expected electron density of densely packed alkyl tails ( $0.3$ – $0.33 e/\text{Å}^3$ ) even considering the uncertainties of the fitting procedure. This difference indicates the presence of additional defects in monolayer structure such as interdomain boundaries or partial conformational disorder.

At the highest surface pressure the length of the topmost box, assigned to the terminal alkyl tails ( $l_{\text{ref}}$ ) is much smaller than the calculated extended length of the tails ( $l_{\text{max}} = 15.2 \text{ Å}$ ) (Table 1). This difference indicates that the alkyl tails are significantly tilted toward the surface. A measure for the tilt,  $\theta$ , estimated from relation  $\cos \theta = l_{\text{ref}}/l_{\text{max}}$  yielding a tilt angle of about  $60^\circ$ . Apparent reason for such highly tilted, almost flat arrangement of the alkyl tails in the compound studied is the availability of a large surface area for a single tail ( $43 \text{ Å}^2$ ) caused by the bulky crown ether group beneath the alkyl layer. This large tilt is unusual for alkyl chains within Langmuir monolayers. Typical tilting angle for amphiphilic organic compounds with alkyl tails is close to  $10$ – $30^\circ$  in condensed solid state.<sup>26,27</sup> This tilt is related to a modest mismatch of cross-sectional areas of nonbulky polar heads (usually, carboxyl groups) and hydrocarbon chains.

Diffraction experiments provided additional insight into the molecular packing of alkyl tails within Langmuir monolayers (Figure 4). The monolayer at lower pressures showed little ordering as indicated by the presence of only a wide diffuse halo, originated from the water subphase. Two-dimensional Bragg reflections do not appear in the diffraction patterns at pressures of 3 and 10 mN/m. XGID scans reveal three peaks only at the highest surface pressures tested here of about 20 mN/m. The peak profiles obtained with high resolution at the highest pressure (Figure 4b) were fitted to Lorentzian type functions that provided peak positions at 1.00, 1.43, and  $1.59 \text{ Å}^{-1}$ , which correspond to 6.26, 4.40, and  $3.94 \text{ Å}$   $d$  spacings, respectively (Table 2).

The shape, spacing, and location of the two intense peaks with higher  $Q_{xy}$  values ( $1.43$  and  $1.59 \text{ Å}^{-1}$ ) correspond closely with literature values for (1,1) and (2,0) planes in an orthorhombic unit cell of alkyl chains.<sup>28</sup> Calculations with this indexation resulted in a unit cell size of  $7.88 \text{ Å}$  by  $5.29 \text{ Å}$  (Figure 5). This unit cell corresponds to a cross-sectional area of  $20.8 \text{ Å}^2$  per alkyl chain of the molecule. This value is within the known area for densely packed and tilted alkyl tails (from 18.2

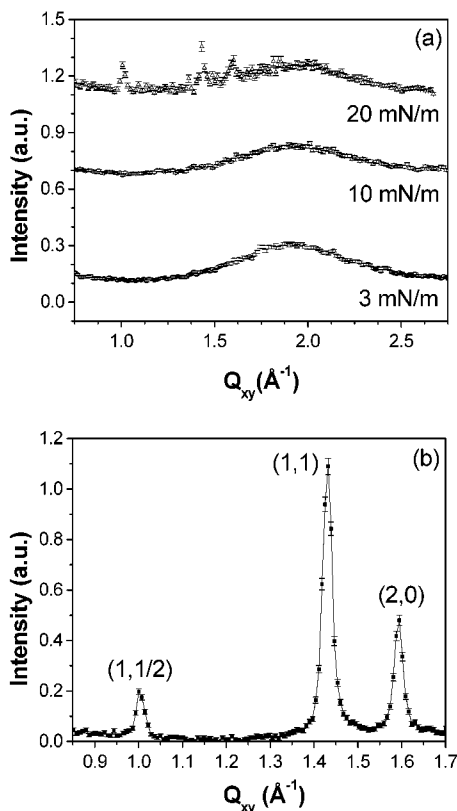


**Figure 4.** (a) Diffraction curves for the **AD12-1** monolayer at three different pressures. (b) High-resolution diffraction scan (after background subtraction) at the highest surface pressure. Characteristic peaks for the (1,1/2), (1,1), and (2,0) planes are labeled.

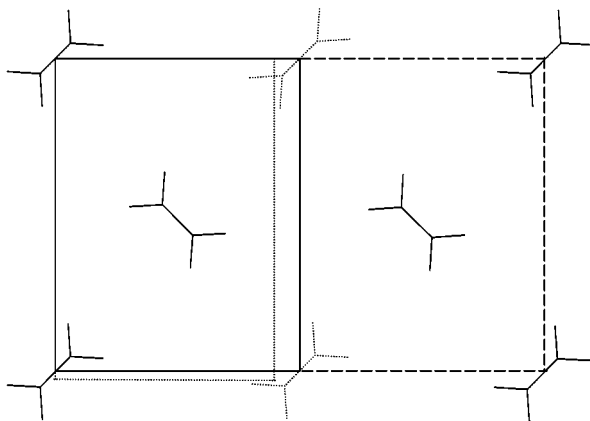


**Figure 5.** Comparison of proposed orthorhombic unit cell and a unit cell from literature. The **AD12-1** orthorhombic unit cell is represented by the solid lines ( $5.29 \times 7.88 \text{ \AA}$ ). The short dashed lines represent the literature unit cell for heneicosanoic acid ( $4.92 \times 7.93 \text{ \AA}$ ).<sup>27</sup> The long dashed line represents the supercell of  $10.58 \times 7.88 \text{ \AA}$  proposed for the molecule studied.

**TABLE 2: Structural Parameters of Molecular Packing Deducted from Diffraction Data and Rod-Scan Experiments**

|                        | peak 1 | peak 2 | peak 3 |
|------------------------|--------|--------|--------|
| d-spacing (Å)          | 6.28   | 4.40   | 3.94   |
| length (Å)             | 15.2   | 15.2   | 15.2   |
| correlation length (Å) | 192    | 165    | 171    |
| tilt angle (deg)       | 54.3   | 58.0   | 56.6   |
| roughness (Å)          | 2.1    | 2.4    | 3.4    |

to  $21.0 \text{ \AA}^2$ .<sup>28-30</sup> However, the  $6.26 \text{ \AA}$  peak with lower intensity detected at this pressure does not fit a simple orthorhombic unit cell common for the alkyl tails.

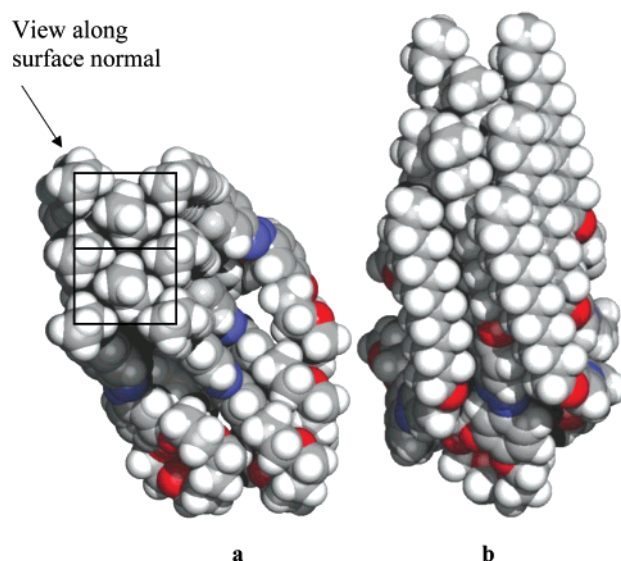


**Figure 6.** Molecular models of molecular packing within the unit cell proposed as viewed along the alkyl chains (a) and top view of monolayer surface covered with highly tilted alkyl tails (b).

After careful analysis of possible structural models, we suggest that this peak corresponds to the formation of a supercell packing shown in Figure 5. Our proposition is based on the fact that the  $d$  spacing for this peak has a simple fractional relationship that corresponds to the (1,1/2) index within the orthorhombic unit cell. The position of the (1,1/2) peak calculated using the orthorhombic unit cell parameters ( $a^* = 2\pi/a = 0.7973 \text{ \AA}^{-1}$  and  $b^* = 2\pi/b = 1.1877 \text{ \AA}^{-1}$ ) is found to be  $0.99 \text{ \AA}^{-1}$ , which is within the experimental uncertainty of the observed value  $1.00 \text{ \AA}^{-1}$ . The appearance of the (1,1/2) peak suggests that  $b$ -direction includes two of the “primary” unit cells as seen in Figure 5. In addition, comparison of the unit cell for **AD12-1** compound studied here with the common unit cell for alkyl chains, namely, heneicosanoic acid found in the literature, demonstrates that **AD12-1** compound possess expanded dimension in the  $b$ -direction.<sup>28</sup>

The cause of the supercell packing structure can be attributed to the influence of the large polar head, which can be misaligned in the  $b$ -direction so that the actual repeating unit is seen in every other unit cell. Indeed, as molecular modeling showed, for tilted and densely packed alkyl tails it was impossible to densely pack all polar fragments with the same orientation. Space constraints required a minor misalignment of alkyl tails to provide the appropriate packing density (Figure 6). We conclude that space constraints imposed by chemical attachment of the alkyl chains to the bulky polar heads appears to be the origin of the supercell of the alkyl tails. A top view projection of the monolayer shows that the alkyl chains appear to be lying almost flat on top of the polar fragments, thus, covering large surface area generated by the bulky polar heads (Figure 6). Indeed, an alkyl tail with the cross-sectional area of  $21 \text{ \AA}^2$  cover nearly  $42 \text{ \AA}^2$  of underlying surface area when tilted  $58^\circ$  from the surface normal (Figure 6).

Independent confirmation of a highly tilted alkyl chains within monolayer at the highest surface pressure came from out-of-plane diffraction studies. As we observed for diffraction data collected at an angle  $\beta = 3.5^\circ$ , the (1,1) peak disappears while the other two peaks remain visible, although with weaker intensity (not shown). This qualitatively confirms tilting of the alkyl chains in (1,1) direction. Rod scans (scanning out-of-plane ( $\beta$  angle) whereas fixing the  $Q_{xy}$  at a peak position) were used to determine the tilt angle of the molecular fragments with better

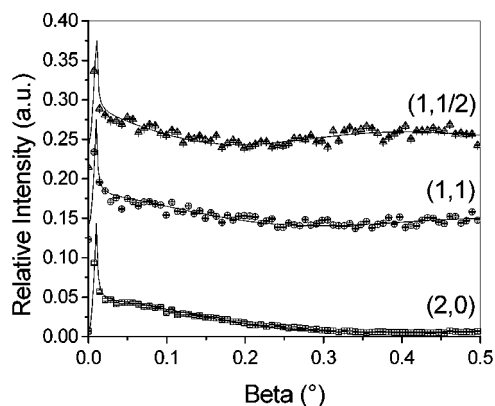


**Figure 7.** Rod scans for different the diffraction peaks labeled with the Miller indices of the equivalent peaks. The data are represented by the symbols while the corresponding best fits are displayed as lines. The intensity for the scans along (1,1) and (1,1/2) directions were increased five times and offset from original data for clarity.

accuracy.<sup>19</sup> For all three diffraction peaks, rod scans displayed angular behavior with a sharp spike in intensity at a exceedingly low angle followed by gradually decreasing intensity (Figure 7). Modeling of these data confirmed the molecular tilting of alkyl chains in a preferred direction. The fitting suggests the alkyl tails are tilted toward their next nearest neighbor at an angle in the range from 54 to 58° (Table 2). The tilting angle obtained from rod scans was virtually identical to one obtained from the reflectivity data (58°) within the uncertainties of both measurements ( $\pm 2^\circ$ ).

To characterize the extension of alkyl chain ordering within the monolayer, we used correlation lengths calculated within Lorentzian approximation. The correlation length ( $\xi$ ) was determined for all three peaks seen in the diffraction pattern using eq 4<sup>31,32</sup>

$$\xi = 2/\Delta \quad (4)$$

where  $\Delta$  is the full width at half-maximum of the Lorentzian peak in units of  $\text{\AA}^{-1}$ . For all three diffraction peaks, the correlation lengths determined to be in the range from 165 to 192  $\text{\AA}$  are close to the resolution limit of our instrument (about 200  $\text{\AA}$ ) (Table 2). Thus, these values represent the estimation of the lowest limit propagation of order. These high values indicate that ordering on the air/water interface at the highest surface pressure far exceeds short-range order common for liquidlike packing of molecules in fluid or partially disordered states.<sup>32</sup> The tails are much more ordered and do form ordered regions which include at least 40 unit cells that corresponds to long-range positional ordering.

Figure 8 demonstrates a side view of the proposed molecular model of the compound studied at the air–water interface at higher surface pressure with all major parameters revealed independently from a combination of X-ray reflectivity, diffraction, and rod-scan data. The alkyl tails appear densely packed with a large degree of tilt from the surface normal reaching 58°. The tails pack in a supercell, which represents doubling of the conventional orthorhombic unit cell of densely packed alkyl tails. Positional ordering of the alkyl tails is expanded over 40 unit cells. We suggest that space constraints imposed by attachment of the alkyl tails to densely packed bulky polar groups located beneath the alkyl layer cause the formation of supercell structure of the alkyl tail unit cell. Water molecules partially surround the azobenzene and the crown head indicated in the model as a partial submerging of these fragments.

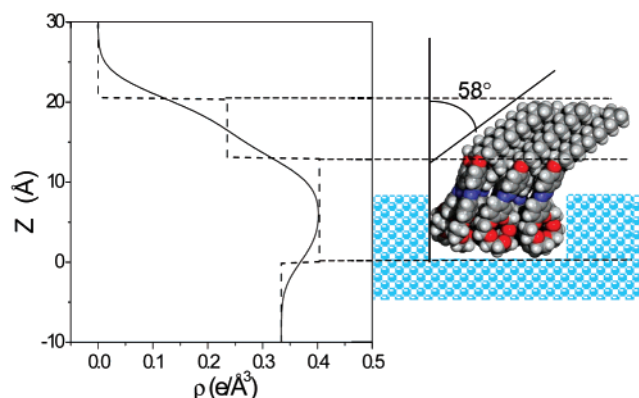


**Figure 8.** Model of molecular packing of AD12–1 molecules at the air–water interface along with the corresponding electron density distribution.

The role of the cross-sectional mismatch between polar heads and alkyl tails has been addressed for amphiphilic compounds with variable number of tails and different polar groups.<sup>33–35</sup> It was considered that a first step in balancing this mismatch was the increase of the surface area covered by the alkyl tails by a tilt of the chains to  $A_0/\cos \theta$ . This resulted in the elongation of the lattice formed by the alkyl tails in one (tilting) direction. Typical tilting angles, however, did not exceed 25–30° for conventional amphiphilic molecules. Then, above some tilting limits, additional distortion of the chain packing was required to satisfy constraints imposed by the headgroup lattice.<sup>33</sup> For larger headgroups, significant expansion of the lattice in the direction perpendicular to the tilting azimuth is expected. Below some spatial limits (estimated to be 8.7  $\text{\AA}$  for the next-to-next neighbor distance for tilting angles below 40°), the adaptation of the mismatch through tilting mechanism was still possible. In lieu of these results, we can conclude that for exceedingly larger headgroups of crown ethers with the diameter of about 10.5  $\text{\AA}$  even extreme tilting of the alkyl chains to about 60° does not completely compensate for the misfit of the alkyl chain packing and the headgroup lattice. Apparent “escape” for the molecules from this situation is the doubling of the effective spacing in the a-direction to 10.58  $\text{\AA}$ , thus accommodating the full diameter of the polar head and creating “supercell” packing for the alkyl tails with some of the chains misaligning or otherwise distorting from their “correct” position to accommodate the polar head lattice.

It is worth to note that the nature of these structural changes is similar to reorganizations observed for surfactant molecules forming micellar structures in solutions.<sup>36–38</sup> As revealed by neutron scattering, increasing the number of ethylene oxide units in polar heads caused increasing stability of spherical micelles and a less favorable situation for rod and lamellar aggregation. At some point, the possibility of bending of the alkyl chains was proposed to accommodate head–tail balance for surfactants with exceedingly large polar heads.<sup>37</sup> Obviously, that for Langmuir monolayers studied here, the molecular organization is constrained to the overall planar morphology without the possibility for complete structural reorganization even if head–tail mismatch favorites it. As a result, extreme tilting of the alkyl chains and breaking the initial symmetry of their packing occur. These are apparent frustrations of local packing compromising between a trend to form nonplanar aggregates and planar Langmuir monolayer constraints.

**Acknowledgment.** The authors thank Dr. A. Sidorenko, M. Lemieux, N. Stephenson, and Dr. Myongssoo Lee for technical

assistance during experiments. Funding from the National Science Foundation, DMR-0074241 including REU supplement for N. Stephenson, is gratefully acknowledged. The Midwest Universities Collaborative Access Team (MUCAT) sector at the APS is supported by the U.S. Department of Energy, Basic Energy Sciences, Office of Science, through the Ames Laboratory under Contract No. W-7405-Eng-82. Use of the Advanced Photon Source was supported by the U.S. Department of Energy, Basic Energy Services, Office of Science, under Contract No. W-31-109-Eng-38.

## References and Notes

- (1) Newkome, G. R.; Moorefield, C. N.; Vogtle, F., Eds. *Dendritic Molecules*; VCH: Weinheim, 1996.
- (2) Frechet, J. M. *Science* **1994**, *263*, 1711.
- (3) Tully, D. C.; Frechet, J. M. *J. Chem. Communications* **2001**, 1229.
- (4) Kampf, J. P.; Frank, C. W. *Langmuir* **1999**, *15*, 227.
- (5) Sayed-Sweet, Y.; Hedstrand, D. M.; Spinder, R.; Tomalia, D. A. *J. Mater. Chem.* **1997**, *7*, 1199.
- (6) Percec, V.; Cho, W. D.; Mosier, P. E.; Ungar, G.; Yearley, D. J. *P. J. Am. Chem. Soc.* **1998**, *120*, 11 061.
- (7) Balagurusamy, V. S. K.; Ungar, G.; Percec, V.; Johansson, G. *J. Am. Chem. Soc.* **1997**, *119*, 1539.
- (8) V. Percec, C. H. Ahn, W. D. Cho, A. M. Jamieson, J. Kim, T. Leman, M. Schmidt, M. Gerle, M. Moller, S. A. Prokhorova, S. S. Sheiko, S. Z. D. Cheng, A. Zhang, G. Ungar, D. J. P. Yearley, *J. Am. Chem. Soc.* **1998**, *120*, 8619.
- (9) Forester, S.; Newbert, I.; Schuler, A. D.; Lindner, P. *Macromolecules* **1999**, *32*, 4043.
- (10) Bo, Z.; Zhang, C.; Severin, N.; Rabe, J.; Schluter, A. D. *Macromolecule* **2000**, *33*, 2688.
- (11) Hashemzadeh, M.; McGrath, D. V. *Am. Chem. Soc., Div. Polym. Chem., Prepr.* **1998**, *39*, 338.
- (12) Sidorenko, A.; Houphouet-Boigny, C.; Villavicencio, O.; Hashemzadeh, M.; McGrath, D. V.; Tsukruk, V. V. *Langmuir* **2000**, *16*, 10 569.
- (13) Tsukruk, V. V.; Luzinov, I.; Larson, K.; Li, S.; McGrath, D. V. *J. Mater. Sci. Lett.* **2001**, *20*, 873.
- (14) Peleshanko, S.; Sidorenko, A.; Larson, K.; Villavicencio, O.; Ornatka, M.; McGrath, D. V.; Tsukruk, V. V. *Thin Solid Films* **2002**, *406*, 233.
- (15) Percec, V.; Johansson, G.; Ungar, G.; Zhou, J. *J. Am. Chem. Soc.* **1996**, *118*, 9855.
- (16) Larson, K.; Vaknin, D.; Villavicencio, O.; McGrath, D. V.; Tsukruk, V. V. *J. Phys. Chem.*, submitted.
- (17) Bohm, C.; Leveiller, F.; Jacquemain, D.; Mohwald, H.; Kjaer, K.; Als-Nielsen, J.; Weissbuch, I.; Leiserowitz, L. *Langmuir* **1994**, *10*, 830.
- (18) Weissbuch, I.; Leveiller, F.; Jacquemain, D.; Kjaer, K.; Als-Nielsen, J.; Leiserowitz, L. *J. Phys. Chem.* **1993**, *97*, 12 858.
- (19) Vaknin, D.; Kelley, M. S. *Biophys. J.* **2000**, *79*, 2616.
- (20) Vankin, D. In *Methods of Materials Research*; Kaufmann, E. N., Abbaschian, R., Barnes, P. A., Bocarsly, A. B., Chien, C. L., Doyle, B. L., Fultz, B., Leibowitz, L., Mason, T., Sanchez, J. M., Eds.; John Wiley & Sons: New York, 2001, p 10d.2.1.
- (21) Gregory, B. W.; Vaknin, D.; Gray, J. D.; Ocko, B. M.; Stroeve, P.; Cotton, T. M.; Struve, W. S. *J. Phys. Chem. B* **1997**, *101*, 2006.
- (22) Hosemann, R.; Bagchi, S. N. *Direct Analysis of Diffraction by Matter*; Interscience: New York, 1962.
- (23) Kaganer, V. M.; Osipov, M. A.; Peterson, I. R. *J. Chem. Phys.* **1993**, *98*, 3512.
- (24) Gaines, G. L. Jr. *Insoluble Monolayers at Liquid-Gas Interfaces*; Interscience: New York 1966.
- (25) Peterson, I. R. *J. Phys. D: Appl. Phys.* **1990**, *23*, 379.
- (26) Pao, W. J.; Stetzer, M.; Heiney, P.; Cho, W. D.; Percec, V. *J. Phys. Chem. B* **2001**, *105*, 2170.
- (27) Kaganer, V. M.; Peterson, I. R.; Kenn, R. M.; Shih, M. C.; Durbin, M.; Dutta, P. *J. Chem. Phys.* **1995**, *102*, 9412.
- (28) Peterson, I. R.; Russell, G. J.; Earls, J. D.; Girling, I. R. *Thin Solid Films* **1988**, *161*, 325.
- (29) Kaganer, V. M.; Mohwald, H.; Dutta, P. *Rev. Mod. Phys.* **1999**, *71*, 779.
- (30) Ulman, A. *An Introduction to Ultrathin Organic Films*; Academic Presses: San Diego, CA, 1991.
- (31) Steitz, R.; Peng, J. B.; Peterson, I. R.; Gentle, I. R.; Kenn, R. M.; Goldmann, M.; Barnes, G. T. *Langmuir* **1998**, *14*, 7245.
- (32) Gunier, A. *X-ray Diffraction In Crystals, Imperfect Crystals, and Amorphous Bodies*; Dover: New York, 1994.
- (33) Tsukruk, V. V.; Shilov, V. *Structure of Polymeric Liquid Crystals*; Kiev: Naukova Dumka, 1990.
- (34) Weidemann, G.; Brezesinski, G.; Vollhardt, D.; Mohwald, H. *Langmuir* **1998**, *14*, 6485.
- (35) Weidemann, G.; Brezesinski, G.; Vollhardt, D.; DeWolf, C.; Mohwald, H. *Langmuir* **1999**, *15*, 2901.
- (36) Sirota, E. B. *Langmuir* **1997**, *13*, 3849.
- (37) Maccarini, M.; Briganti, G. *J. Phys. Chem. A* **2000**, *104*, 11 451.
- (38) Haldar, J.; Aswai, V. K.; Goya, P. S.; Bhattacharya, S. *J. Phys. Chem. B* **2001**, *105*, 12 803.
- (39) Won, Y.-Y.; Davis, H. T.; Bates, F. S.; Agamalian, M.; Wignall, G. D. *J. Phys. Chem. B* **2000**, *104*, 7134.